Supporting Information for Band-Like Charge Transport in $Cs_2AgBiBr_6$ and Mixed Antimony-Bismuth $Cs_2AgBi_{1-x}Sb_xBr_6$ Halide Double Perovskites

Eline M. Hutter*,[†‡] María C. Gélvez-Rueda,[‡] Davide Bartesaghi,[‡] Ferdinand C. Grozema,[‡] and Tom J. Savenije*[‡]

†. Department of Chemistry, Stanford University, Stanford, California 94305, United States

‡. Department of Chemical Engineering, Delft University of Technology, Van der Maasweg 9, 2629 HZ Delft, The Netherlands

* E.M.Hutter@tudelft.nl

* T.J.Savenije@tudelft.nl

Table S1: XPS elemental analysis of $Cs_2AgBi_{1-x}Sb_xBr_6$ powders.

x		% Cs	% Ag	% Bi	% Sb	% Br	Sb/(Sb+Bi)
0	*spot 1*	34.26	8.67	8.79	0.09	48.20	0.010
	spot 2	26.09	6.06	8.30	0.03	59.52	0.004
	average	30.18	7.37	8.55	0.06	53.86	**0.007**
0.05	*spot 1*	24.60	9.14	7.62	0.66	57.97	0.080
	spot 2	25.28	10.21	7.10	0.42	57.00	0.056
	average	24.94	9.68	7.36	0.54	57.49	**0.068**
0.1	*spot 1*	25.57	8.91	7.06	1.66	56.80	0.190
	spot 2	26.00	8.85	6.56	1.51	57.09	0.187
	average	25.79	8.88	6.81	1.59	56.95	**0.189**
0.4	*spot 1*	24.41	9.32	5.00	3.73	57.54	0.427
	spot 2	25.09	9.11	4.85	3.80	57.15	0.439
	average	24.75	9.22	4.93	3.77	57.35	**0.433**

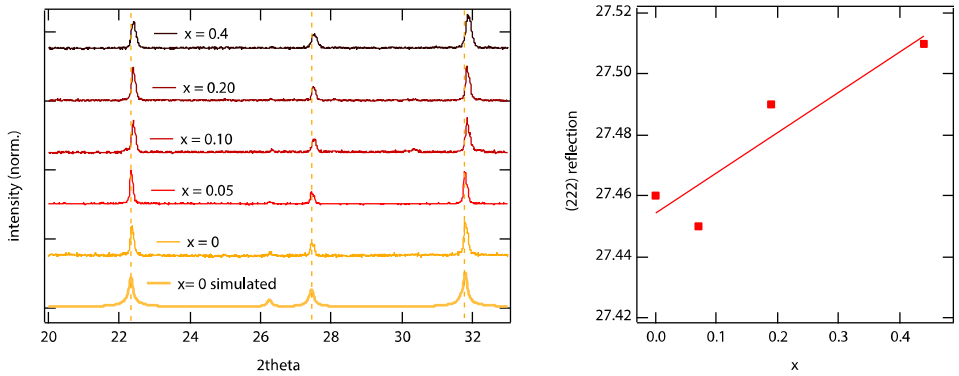

Figure S1: (a) Zoom-in of the X-Ray Diffraction patterns of $Cs_2AgBi_{1-x}Sb_xBr_6$ from **Figure 1b**. The yellow dotted lines indicate the positions of the (022), (222) and (004) reflections, respectively, for $Cs_2AgBiBr_6$, showing that these shift to larger 2θ values for increasing *x*. This confirms that the lattice contracts on replacing Bi with the smaller Sb. (b) 2θ value of (222) reflection as function of Sb-content (using the *x* values from Table S1).

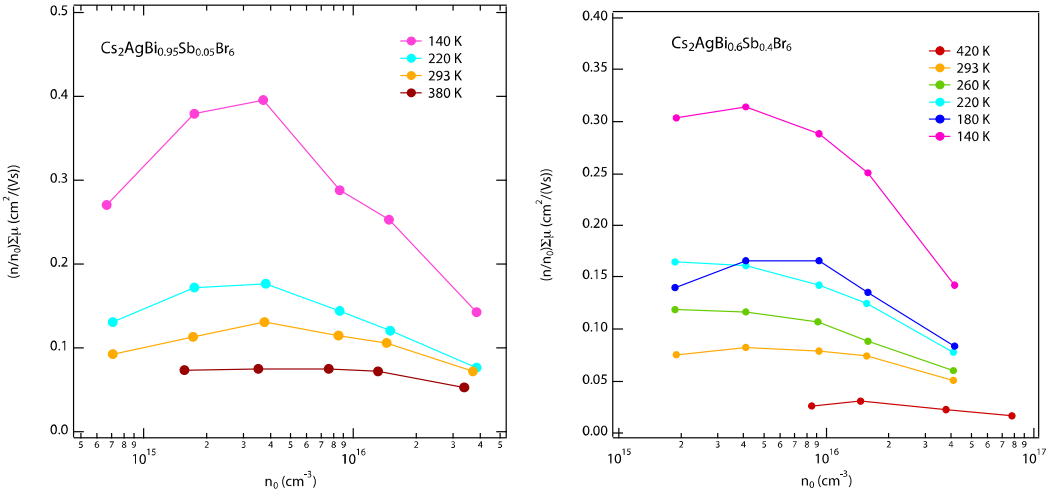

Figure S2: $(n/n_0)\sum\mu$ as function of n_0 and temperature for $Cs_2AgBi_{1-x}Sb_xBr_6$ with x = 0.05 (left) and x = 0.4 (right). Similar to the data shown in Figure 2b in the main text, we used the maximum $(n/n_0)\sum\mu$ at each temperature to estimate the trap saturation density, which is shown in Figure 2c. Note that for $Cs_2AgBi_{0.6}Sb_{0.4}Br_6$, at 220 K and higher the $\sum\mu$ (T) is nearly flat up to ~4 x 10^{15} cm^{-3}, suggesting that trap saturation occurs at or below the lowest densities used for the measurements.

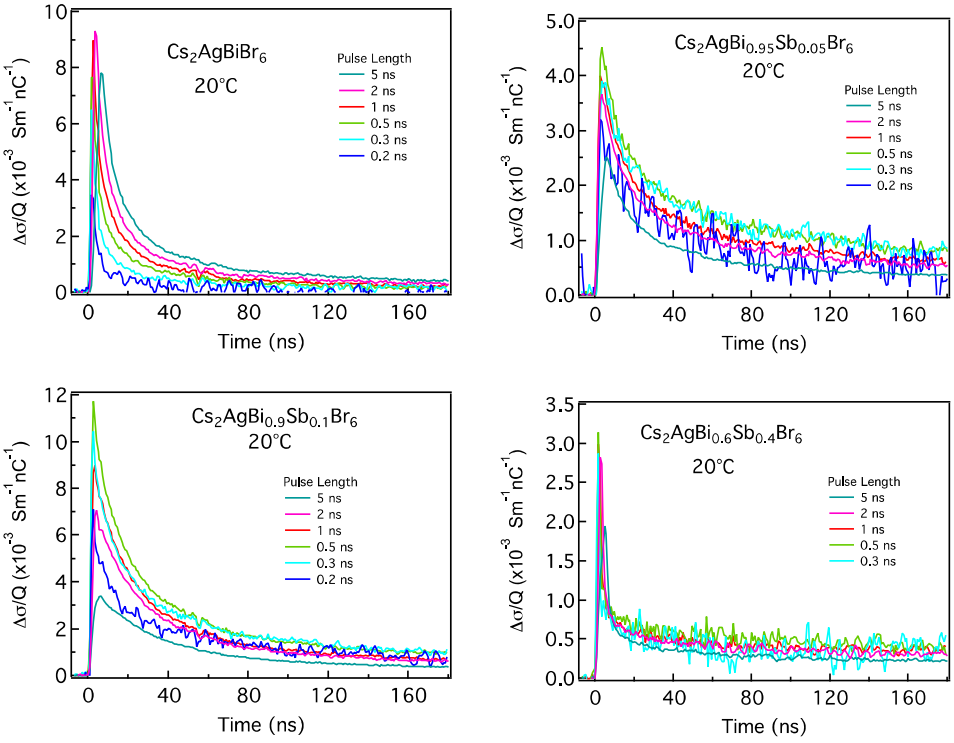

Figure S3: PR-TRMC lifetimes for the different $Cs_2AgBi_{1-x}Sb_xBr_6$ powders.

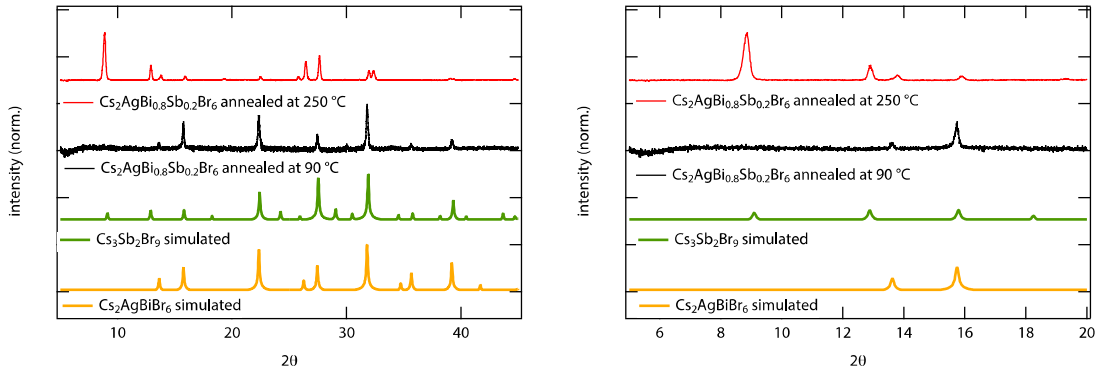

Figure S4: (a) X-Ray Diffraction patterns of thin films prepared from spin-coating $Cs_2AgBi_{0.8}Sb_{0.2}Br_6$ (0.5 M in DMSO), followed by annealing at 250 ºC (red) and at 90 ºC (black) and (b) zoom-in of the patters shown in (a). These results show that the HDP crystal structure is preserved at low annealing temperatures, whereas high annealing temperatures lead to the formation of undesired side phases (such as $Cs_3Sb_2Br_9$).

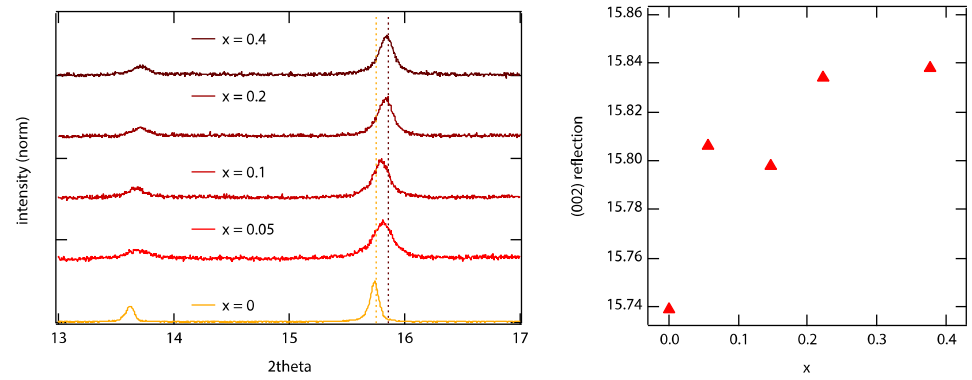

Figure S5: (a) Zoom-in of the X-Ray Diffraction patterns of $Cs_2AgBi_{1-x}Sb_xBr_6$ from **Figure 3a**. The yellow and dark red dotted line indicate the positions of the (002) reflections for $Cs_2AgBiBr_6$ and $Cs_2AgBi_{0.6}Sb_{0.4}Br_6$, respectively, showing that these shift to larger 2θ values for increasing *x*. This confirms that the lattice contracts on replacing Bi with the smaller Sb. (b) 2θ value of (002) reflection as function of *x*, using the values from Table S2.

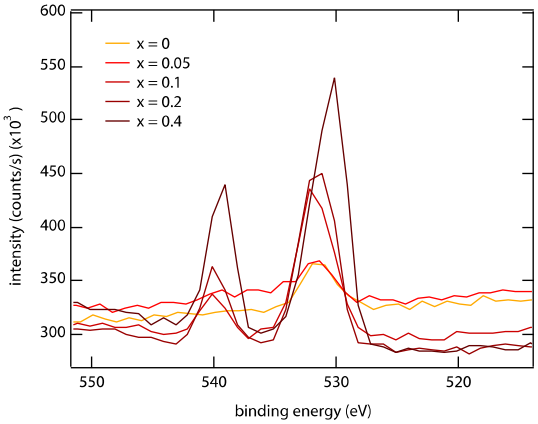

Figure S6: Zoom-in of X-ray photoelectron spectra of $Cs_2AgBi_{1-x}Sb_xBr_6$ thin films, with x = 0, 0.05, 0.1, 0.2, 0.4. The peaks at 540 eV and 531 eV are characteristic for Sb; the (small) additional peak observed at 531 eV for x = 0 originates from oxygen.

Table S2: XPS elemental analysis of $Cs_2AgBi_{1-x}Sb_xBr_6$ thin films.

x		% Cs	% Ag	% Bi	% Sb	% Br	Sb/(Sb+Bi)
0	*spot 1*	21.93	6.84	6.81	0.03	64.39	0.004
	spot 2	23.18	7.15	8.39	0.05	61.22	0.006
	average	22.56	7.00	7.60	0.04	62.81	**0.005**
0.05	*spot 1*	21.48	9.11	8.69	0.21	60.50	0.024
	spot 2	19.05	12.03	13.73	1.31	53.87	0.087
	average	20.27	10.57	11.21	0.76	57.19	**0.055**
0.1	*spot 1*	20.29	9.89	7.27	1.21	61.34	0.143
	spot 2	28.01	10.39	9.20	1.65	50.76	0.152
	average	24.15	10.14	8.24	1.43	56.05	**0.147**
0.2	*spot 1*	21.33	7.76	7.24	2.08	61.59	0.223
	spot 2	22.86	9.79	7.88	2.27	57.20	0.224
	average	22.10	8.78	7.56	2.18	59.40	**0.223**
0.4	*spot 1*	21.97	8.47	5.51	4.00	60.05	0.421
	spot 2	23.28	15.38	11.37	5.73	44.24	0.335
	average	22.63	11.93	8.44	4.87	52.15	**0.378**

Table S3: Diffusion lengths calculated from the time at which half of the charges is immobilized, *i.e.* the half lifetime, and the mobilities both obtained from the photoconductivity (thin films) measurements using an excitation intensity leading to an initial concentration of 3 - 6 x 10^{16} cm^{-3}.

$Cs_2AgBi_{1-x}Sb_xBr_6$	half lifetime (ns)	mobility (cm^2/(Vs))	L_D (nm)
x = 0	260	0.65	662
x = 0.2	172	8.6E-04	20
x = 0.4	98	6.0E-03	39

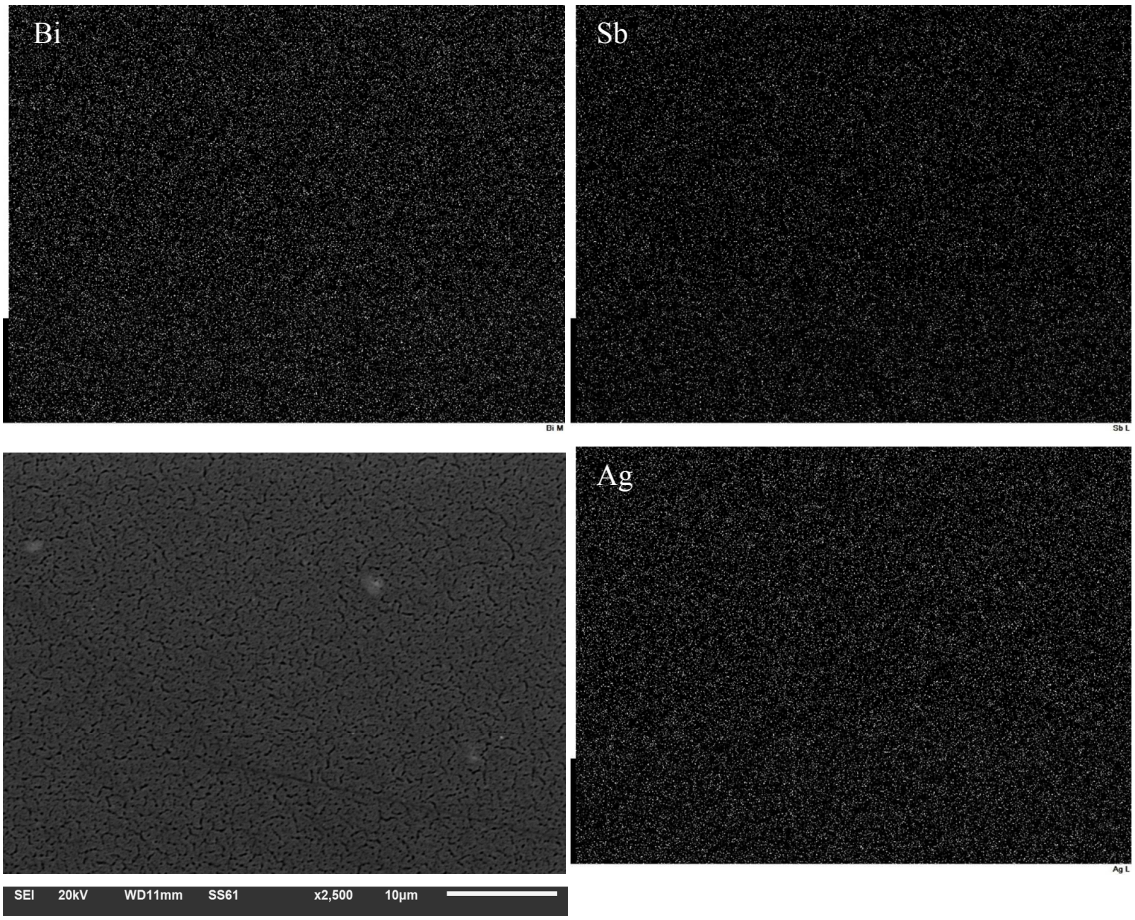

Figure S7: Scanning Electron Microscopy image of the $Cs_2AgBi_{0.6}Sb_{0.4}Br_6$ thin film and corresponding EDS elemental analysis maps for Sb, Bi and Ag.

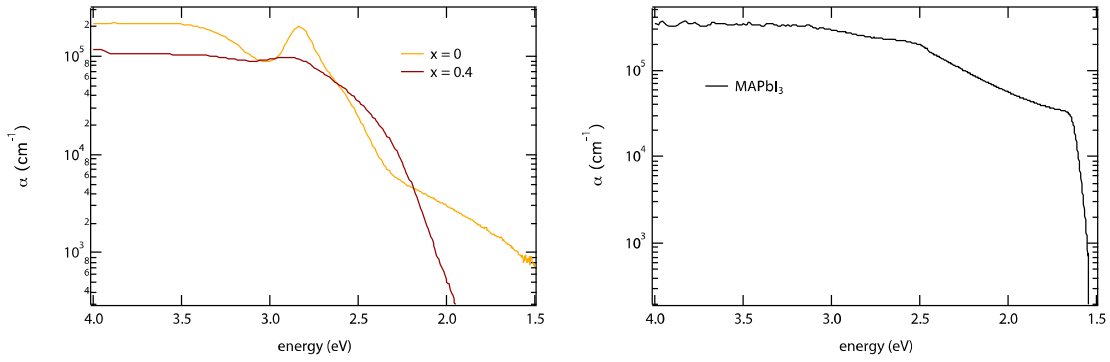

Figure S8: Energy-dependent absorption coefficient for $Cs_2AgBi_{1-x}Sb_xBr_6$ with x = 0 and 0.4, determined from the absorption and transmission spectra of the thin films, recorded using an integrating sphere. The absorption coefficient of methylammonium lead iodide ($MAPbI_3$), data from Ref. [1], is shown for comparison.

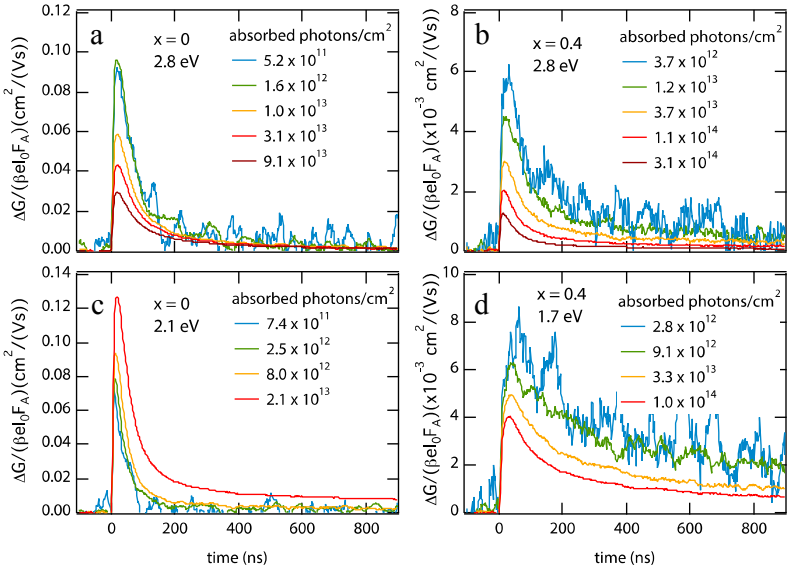

Figure S9: (a-d) Intensity-normalized photo-conductance traces for powder samples as function of time at an excitation energy of 2.8 eV for $x = 0$ (a) and $x = 0.4$ (b) and at 2.1 eV for $x = 0$ (c) and 1.7 eV for $x = 0.4$ (d).

References:

(1) Hutter, E. M.; Gélvez-Rueda, M. C.; Osherov, A.; Bulović, V.; Grozema, F. C.; Stranks, S. D.; Savenije, T. J. *Nat. Mater.* **2017**, *16* (1).